Time-resolved changes in equatorial x-ray diffraction and stiffness during rise of tetanic tension in intact length-clamped single muscle fibers

G. Cecchi,* P. J. Griffiths,‡ M. A. Bagni,* C. C. Ashley,‡ and Y. Maeda

European Molecular Biology Laboratory, Hamburg Outstation, Deutsches Elektronen-Synchrotron, W-2000 Hamburg 52, Germany; *Dipartmento di Scienze Fisiologiche, Universita degli Studi di Firenze, Florence I-50134, Italy; ‡University Laboratory of Physiology, Oxford OX1 3PT, United Kingdom

ABSTRACT We report the first time-resolved x-ray diffraction studies on tetanized intact single muscle fibers of the frog. The 10, 11, 20, 21, 30, and Z equatorial reflections were clearly resolved in the relaxed fiber. The preparation readily withstood 100 1-s duration (0.4-s beam exposure) tetani at 4°C (<4% decline of force and no deterioration in the 10,11 equatorial intensity ratio at rest or during activation).

Equatorial intensity changes (10 and 11) and fiber stiffness led tension ($t_{1/2}$ lead 20 ms at 4°C) during the tetanus rise and lagged during the isometric phase of relaxation. These findings support the existence of a low force cross-bridge state during the rise of tetanic tension and isometric relaxation that is not evident at the tetanus plateau.

In "fixed end" tetani lattice expansion occurred with a time course similar to stiffness during the tetanus rise. During relaxation, lattice spacing increased slightly, while the sarcomere length remained isometric, but underwent large changes after the "shoulder" of tension. Under length clamp control, lattice expansion during the tetanus rise was reduced or abolished, and compression (2%) of the lattice was observed. A lattice compression is predicted by certain cross-bridge models of force generation (Schoenberg, M. 1980. *Biophys. J.* 30:51–68; Schoenberg, M. 1980. *Biophys. J. 30:69–78).*

INTRODUCTION

The development of active tension in skeletal muscle is believed to involve the formation of transient mechanical connections (cross-bridges) between actin and myosin filaments (Hanson and Huxley, 1955; Huxley, 1957). During a tetanus, single intact frog muscle fibers show an increase in instantaneous stiffness consistent with the formation of parallel elastic linkages between actin and myosin (Huxley and Simmons, 1971), while the interpretation of the equatorial x-ray diffraction pattern of activated whole sartorius from the frog implies a transfer of mass from the region of the myosin to the actin filaments compared with the relaxed state (Haselgrove and Huxley, 1973) as would be expected from the cross-bridge model for force development, within the framework of the sliding filament mechanism (Huxley and Niedergerke, 1954; Huxley and Hanson, 1954).

The time course of changes in stiffness and equatorial reflection intensity (I_{11} and I_{10}) differ from that of force. Both stiffness and equatorial intensity changes lead force during the tetanus rise, and lag during relaxation (Cecchi et al., 1982; Ford et al., 1986; Huxley and Haselgrove, 1977). During the tetanus rise, this could result from initial formation of cross-bridges occurring substantially before tension generation, but alternatively, the lead of stiffness over tension could be explained if stiffness of an individual cross-bridge varied between different attached intermediates of the cross-bridge cycle. It is also not proven that x-ray data and stiffness measurements are detecting the same attached state at the start of a tetanus. To distinguish between these possibilities, we have compared the time course of changes in stiffness, I_{10} and I_{11} in the same preparation. In addition, to obtain the highest quality mechanical data and to eliminate population and variable sarcomere length effects on the x-ray reflections, we have developed a technique which permits the use of an intact single fiber preparation in conjunction with synchrotron radiation ($\lambda = 0.15$ nm) for time-resolved x-ray diffraction studies. The use of this preparation also permits us to apply the "length clamp" technique based upon instantaneous sarcomere length measurement to maintain isometric conditions during the rise of tetanic tension.

In addition to permitting direct comparison of time-resolved x-ray diffraction data with intact single fiber mechanics, these experiments on the intact single fiber preparation provide a framework for the evaluation of time-resolved x-ray diffraction studies on skinned fiber preparations, where the mechanical and x-ray diffraction conditions are more similar to the intact single fiber preparation than to whole muscle. The present results are the first time-resolved x-ray diffraction studies to be reported from an activated intact single muscle fiber preparation from a vertebrate under length clamp control.

Here we report time-resolved changes in lattice spacing during tetani obtained both under fixed-end and length-clamped conditions, and provide evidence in

0006-3495/91/06/1273/11 $2.00

support of previous reports of a low force attached cross-bridge state.

METHODS

1. Muscle fibers

Single muscle fibers were dissected from tibialis anterior muscles of *Rana temporaria*. Aluminum clips were attached to the tendons as close as practically possible to the ends of the cell to reduce tendon compliance. Attachment of the preparation to the length motor and the force transducer was achieved by small hooks on these devices, which were inserted into holes in the aluminum clips. Fiber length was typically 6–7 mm, and fibers were eliptical in cross-section, having a maximum diameter up to 300 μm and a minimum of ~120 μm. Care was taken during mounting to remove any twists in the fiber so as to avoid rotational movement during tetani. Where possible, fibers were orientated with the minor diameter in the plane of the laser beam, since this gave rise to a better quality laser diffraction pattern. Throughout the dissection and the experiment, fibers were bathed in Ringer's solution of composition (in millimolar): NaCl, 115; KCl, 2.5; $CaCl_2$, 1.8; Na_2HPO_4, 2.15; NaH_2PO_4, 0.85 (Adrian, 1956). pH was adjusted to 7.00 ± 0.02, temperature 4.0 ± 0.2°C.

2. Experimental chamber.

The chamber, force transducer, stretcher, and laser optics were mounted on an aluminum bench containing locating screws on its base so that the whole arrangement could be transferred to the dissection site for fiber mounting and then returned to the synchrotron beam line with minimum adjustment of x-ray optics. The experimental chamber consisted of a rectangular well milled into an aluminum block, and contained two Pt mesh stimulating electrodes, one above, the other below the preparation. The use of mesh electrodes permitted incident and diffracted laser light to pass unobstructed through the upper and lower electrodes. All aluminum surfaces inside the well were coated with epoxy. The fiber was suspended horizontally between a capacitance force transducer (resonance frequency 30–50 kHz) and a moving coil stretcher (Huxley and Lombardi, 1980; Cecchi et al., 1976), which projected into the chamber through narrow slots cut into the ends of the well. The base of the chamber was glass, and the chamber was closed with an aluminum lid containing a glass window, so that illumination from below with a HeNe laser via a focusing lens resulted in the projection of the laser diffraction pattern through the glass window in the lid. The lid window was recessed into the aluminum to avoid condensation resulting from cooling, and consequent distortion of the pattern. The angle of incidence of the laser beam at the fiber was adjusted so as to maximize the intensity of the first-order reflection. In the horizontal plane, two adjustable 7-mm-diam Kapton (7.5 μm thick; Du Pont Corp., Wilmington, DE) windows were placed within 0.5 mm of the fiber axis through which the x-ray beam entered the chamber, so as to minimize the path length of the beam through the bathing medium and hence beam scattering. A schematic representation of the experimental set up is shown in Fig. 1.

The position of the stretcher moving coil was servo-controlled using an electronic circuit already described (Cecchi et al., 1976). Fixed-end conditions were obtained by feeding back the output of the photodiode signalling the position of the moving coil. Length-clamped conditions were obtained by feeding back the output of the laser diffractometer so as to hold constant the sarcomere length of the fiber segment illuminated by the laser beam, independent of the length changes undergone by the rest of the fiber. The system could be switched from the fixed end mode to the length-clamped mode and vice versa by a command pulse. For length-clamped tetanus, the system was switched to the length-clamped mode just before the onset of stimulation and returned to fixed end mode just before relaxation.

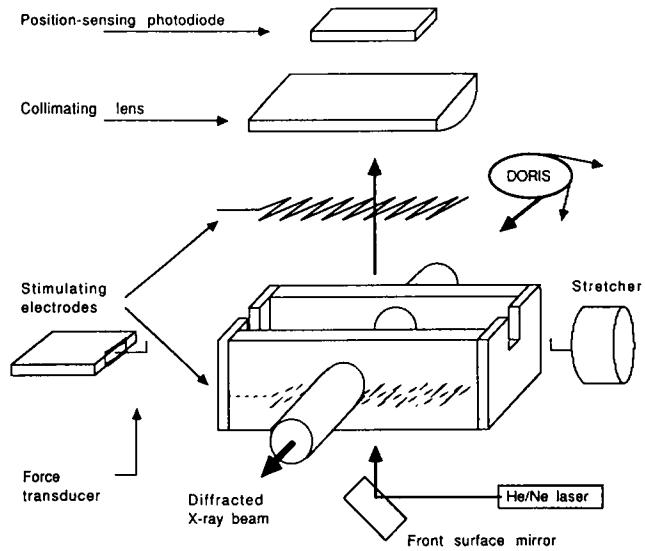

FIGURE 1 Schematic of the experimental apparatus. X-ray radiation (wavelength 0.15 nm) enters and leaves the chamber through the plane of the page. Laser light passes through the glass base of the chamber, then through the grid stimulating electrode at the bottom of the chamber, the fiber, and the grid electrode at the top. After collimation by a cylindrical lens, the first order diffracted beam strikes a position sensing photodiode. During the experiment the chamber is sealed by a lid (not shown) to avoid condensation and to improve the laser pattern.

3. X-ray optics

X-ray diffraction pattern were recorded at station EMBL X-33 situated in the synchrotron laboratory (HASYLAB) of the Deutsches Elektronen Synchrotron (DESY, Hamburg, Germany). The beam line accepts x-ray photons from electrons orbiting the storage ring DORIS. During these experiments, the ring stored only electrons of 50 to 95 mA at 3.656 GeV. The focusing x-ray optics at X-33, consisting of a triangular germanium monochromator focusing in the horizontal plane followed by a totally reflecting segmented quartz mirror that focuses in the vertical plane, has been previously described (Kress et al., 1986; Maeda et al., 1986). The x-ray optics (including slits) were carefully optimized for fine focus (~4 mm wide in the horizontal plane and 0.4 mm vertically) and for the highest possible brightness. Especially the vertical width of the beam on the specimen was chosen to fullfil two requirements; (*a*) the beam is wide enough so that possible movement of the fiber within the beam does not give rise to substantial change in signal size, and (*b*) the beam is small enough to keep the instrumental background low. We found that, by replacing all Beryllium windows downstream from the aperture slits with Kapton windows, the instrumental background was so diminished that the vertical width of the beam (and therefore the flux, which does not irradiate the fiber) may be substantially larger than the diameter of the

preparation. This helped us to reduce the movement artifact associated with contraction.

4. X-ray detector, data aquisition system

X-ray equatorial reflection intensities were recorded with a one-dimensional position counter of the wire-by-wire type (Hendrix et al., 1982) at 3.8 m from the specimen. The detector was operated at 4.7 kV filled with 80:20 Xenon/CO_2 mixture, which was maintained at a pressure of 2.6 atm. The overall efficiency of the system was almost 100%. The detector was placed on the equator behind a slit 10 mm wide that limits the axial aperture either side of the equator, accepting the full axial width of the reflections.

The data aquisition system including the program was previously described (for further references, see Maeda et al., 1986). In brief, a LSI 11/2 auxiliary crate controller controls the data aquisition of both x-ray spectra and analogue data such as sarcomere length (see below). The data are stored in local memory, and subsequently dumped to a VAX 11/750 computer.

5. Sarcomere length and stiffness measurement

After mounting of the chamber at the beam line, the laser beam was aligned so as to illuminate the center of the part of the fiber that was irradiated by the x-ray beam. Above the fiber was mounted a position sensing photodiode that detected the position of the first order laser diffraction band, collimated to a spot by a cylindrical lens. The signal from the photodiode was then converted to sarcomere length using an analogue computer, and was used to drive the stretcher to maintain a constant sarcomere length. Stiffness measurements were made during fixed end contractions by exposure of the fiber to low amplitude ($\sim$0.1% fiber length) high frequency sinusoidal oscillations (4 kHz) when not subjected to length clamp at one end of the fiber, and measurement of the force at the other. The stiffness was then taken to be the ratio of the amplitude of force to length change. At very low forces a phase shift was sometimes detected between length and force signals. This has been explained in terms of fiber resonance (Ford et al., 1978; Cecchi et al., 1986; Eason, 1989), and under such circumstances the oscillation frequency was reduced slightly until the phase shift disappeared.

6. Experimental protocol

To optimize the position of the fiber within the beam, the integrated intensity resting pattern of the fiber was measured as the fiber was raised or lowered by an electric motor until an optimum position was found. During this procedure, the beam was attenuated by aluminum foil so as to reduce fiber exposure. Occasionally even during length clamp some variation of the position of the fiber in the beam occurred, so that the intensities of the reflections contained a movement component. This was evident as a change in total intensity of the diffraction pattern. As a compensation for this effect, integrated intensity of subsequent time frames was normalized to that of the first frame. This was justified by the observation that in fibers showing little shortening during activation, integrated intensity from the x-ray detector was constant within 2%, although there is no theoretical restriction that keeps the integrated intensity constant. Data sets having a movement artifact of 10% or more of the integrated resting intensity were rejected. The fiber was tetanically stimulated at 3-min intervals for 1 s duration using the minimum frequency to obtain a fused tetanus (typically 20 Hz). To obtain a statistically satisfactory data set at 10 ms resolution, it was necessary to average 60 to 100 tetani, depending on fiber size. During this period the fiber showed no sign of deterioration, tension declining by $<4\%$ during the course of an experiment. After each 10 tetani, a resting pattern was recorded from the fiber, and examined to determine fiber condition and positioning in the x-ray beam. In addition, each tetanus was recorded on a digital oscilloscope and compared with the previous response to detect any fiber deterioration.

7. Data analysis

Because of the high time resolution required in the stiffness measurements, force, and length oscillations required a separate data acquisition system, and were therefore recorded by a Nicolet Explorer 2090 digital scope and stored on floppy disks. Initial estimates of equatorial intensity changes were made by subtraction of background scatter under the peaks. This background scatter was estimated either by a polynomial fit to the regions of the diffraction pattern containing no reflections, or by eye using a segment of an exponential curve. Subsequently it was found that data scatter was usually reduced if total area of peaks, including background, was used, and this method has been adopted for the figures presented here. In all experiments, however, the time course of intensity changes was calculated by both methods, with negligible difference between the two observed. Throughout the figures in which 10 intensity is displayed, the changes in intensity of this reflection have been reversed so as to change in the same direction as stiffness and 11 intensity.

Lattice spacing (the center to center distance between adjacent myosin filaments in the myofilament lattice) was calculated by first subtracting a function representing background scatter which gave an adequate fit by eye to the data. The remaining peak, now on a flat base line, was then treated as though each detector channel (128 in total) were divisible into 40 parts. The 40 divisions were then assigned values appropriate to a linear extrapolation between adjacent channel counts, and the total counts (real plus extrapolated) summed over the range of the peak. The point at which the summed counts equaled 50% of the total was determined and taken to be the position of the peak of that particular reflection. This was performed for both 11 and 10 reflections on either side of the zero order reflection, and the lattice spacing calculated according to

$$\alpha = \frac{2L}{x_{11}} = \frac{2L}{x_{10}} \frac{1}{\sqrt{3}}, \tag{1}$$

where L is the camera constant for a particular experiment (typically 5.907×10^{-10} m^2, and x_{10} and x_{11} are the separations of the 10 and 11 reflections, respectively, from the center of the x-ray diffraction pattern. Owing to the broadening of the 11 reflection which accompanied activation, and which caused overlap of this reflection with the Z and the 20 reflections, the lattice spacing calculated from this reflection has not been used in preparation of data presented in this paper.

The x-ray camera was calibrated for the meridional reflection at 1/14.34 nm^{-1} (Haselgrove, 1975), which was recorded on the same set up from the same fiber with the detector rotated onto the meridian. Throughout the text, dimensions associated with the filament lattice are given in nanometers.

Data obtained from initial experiments performed without sarcomere length recording have not been included in the data presented here.

RESULTS

1. Equatorial x-ray diffraction patterns from the resting fiber and at the tetanus plateau

Fig. 2 *a* shows the resting equatorial diffraction pattern from the intact single fiber recorded during a 3-s exposure to the beam. The general features of the 11 and 10 reflections are similar to those described for whole muscle (Yu et al., 1977), but both reflections are clearly defined so that it is possible to identify additional 20, 21, and 30 reflections on the pattern that are not always well resolved in whole muscle work. The small reflection lying immediately outside the 11 peaks in the relaxed spectrum (the *Z* reflection) arises from the square actin filament lattice arrangement at the *Z* line (Yu et al., 1977).

After activation, there was a reversal of relative intensities of the 11 and 10 equatorial reflections, the intensity of the 11 reflection (I_{11}) increased, while that of the 10 reflection (I_{10}) decreased (Fig. 2 *b*). The decrease in I_{10} occurred principally as a reduction in amplitude of the reflection, whereas the increase in I_{11} resulted from an increase in amplitude together with a considerable broadening. The broadening of the 11 reflection usually obscured the 20 and the *Z* reflections. On the whole, the definition of other reflections was reduced during tetani. Our experience was that the majority of fibers survived > 100 tetani with a beam exposure of 400 ms per tetanus without deterioration in equatorial intensity ratio or of force (4% or less), and therefore beam damage is not the limiting factor in this type of experiment.

The sarcomere length dependence of the ratio of I_{10} to I_{11} was examined in the relaxed and activated state (Fig. 3). At a sarcomere length of 2.15 μm we obtain a mean ratio (I_{10}/I_{11}) in the relaxed state of 2.218 ± 0.359 (n = 15). Upon activation, this changed to 0.509 ± 0.069 (n = 13). These values are in good agreement with those reported by Matsubara and Yagi (1978) which were obtained in whole muscle (2.3 in relaxed muscle, 0.53 at the tetanus plateau, sarcomere length 2.2 μm), but somewhat different from those of Haselgrove and Huxley (1973), who obtained ratios of 2.6 and 0.78 for the relaxed and activated states, respectively. Above 2.2 μm sarcomere length, this ratio shows a roughly linear dependence on sarcomere length, in agreement with the

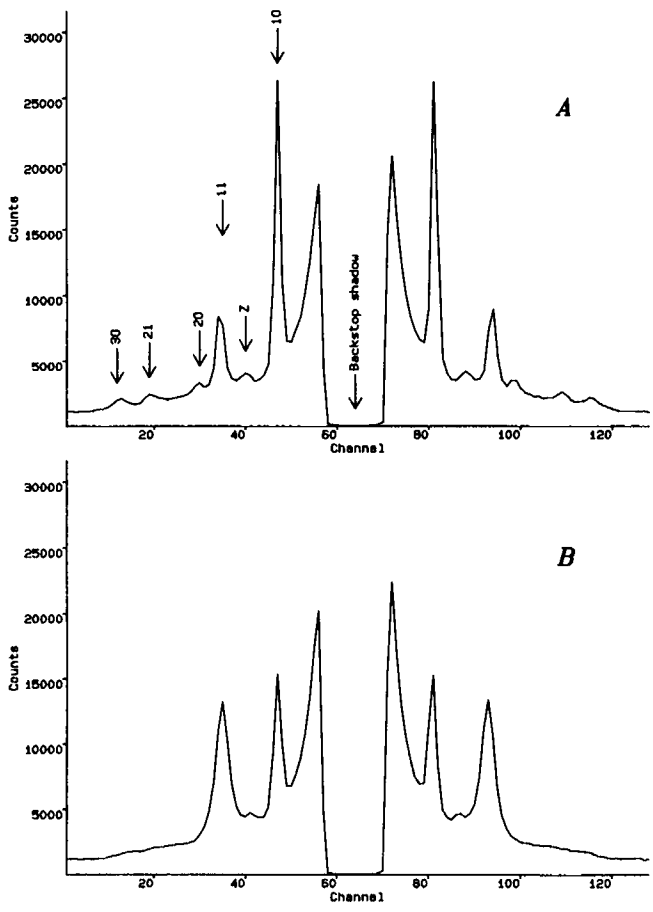

FIGURE 2 Equatorial pattern at rest (*a*) and during the tetanus plateau (*b*). Both patterns from the same fiber. Total exposure time per pattern 3 s. The outer and inner reflections surrounding the 11 reflection in the relaxed state are the 20 and *Z* reflections, respectively. The pair of small outer reflections are the 21 and 30. All of these smaller reflections are less evident in the activated pattern.

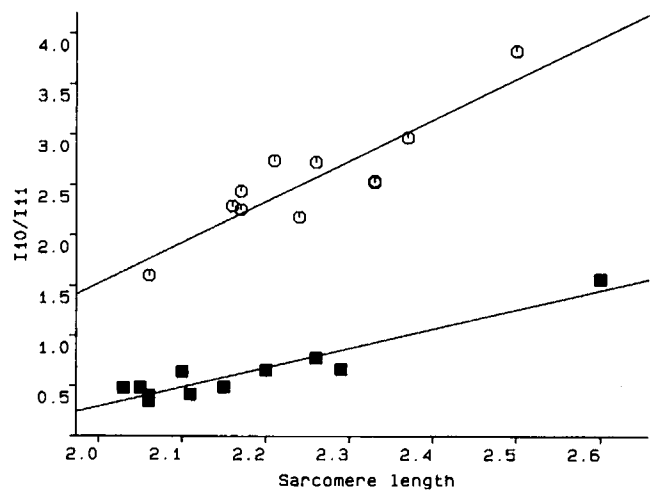

FIGURE 3 The sarcomere length dependence of the I_{10}/I_{11} ratio during the tetanus plateau (■) and at rest (○). Since the relationship seems quasi linear over this range of sarcomere lengths, a linear regression line has been drawn through the points for both sets of conditions.

findings for whole muscle (Elliott et al., 1963; Huxley and Haselgrove, 1973). The ratio in activated fibers as a function of sarcomere length is a roughly constant fraction of the relaxed ratio over the range of sarcomere lengths studied.

2. Intensity changes during activation

Initially these experiments were performed without servo-control of sarcomere length (fixed end tetani), and tetanic tension development was accompanied by a sarcomere shortening of the order of 2–3%. Subsequently the development of the servosystem for use at the beamline permitted reduction of sarcomere length changes during the tetanus rise to <0.3%, and such residual shortening as occurred was completed before force reached 0.1 P_0. Table 1 shows the relative halftimes for changes in stiffness, equatorial intensities and tension for unclamped ("fixed end") and length clamped (isometric) tetani. Because the servo system was unable to follow accurately the small amplitude, high frequency vibrations required for stiffness measurement, these were performed without sarcomere length control. However, previous experiments have shown that under identical conditions of fiber preparation, the ratio of stiffness to tension under clamped conditions did not significantly differ from unclamped conditions (Cecchi et al., 1987). In whole muscle, Kress et al. (1986) reported a $t_{1/2}$ for the increase in I_{11} of 27 ms during the tetanus rise. The corresponding $t_{1/2}$ for force in their experiments was 38 ms. This is somewhat faster than the halftime for force that we obtained (Table 1). However, it seems that the rise of tension in fibers used for study of the time course of equatorial intensity changes by Kress et al. (1986) was anomalously fast compared with the other fibers used in their study, whose time course for the rise of tetanic tension accords much more closely with the values we report here. Taking into account the difference in species of frog used, the choice of muscle, the difference in temperature and possible differences in the extent of cold adaptation of the frogs used in the two studies, we do not consider this difference in force halftimes significant. Our stiffness measurements were usually performed after 40 tetani. Fig. 4 shows the time course of tension and equatorial intensity changes during the rise of tetanic tension in a length-clamped fiber, and stiffness from the same fiber during a fixed end contraction. It is apparent that stiffness and both equatorials have a similar time course, consistent with their detection of the same event. The use of the length clamp had relatively little effect on the time course of the rise of tension. However, it must be borne in mind that our fibers were prepared in a manner that minimized tendon compliance, and it would be inappropriate to assume a negligible effect of length clamping on the time course of tension development in other circumstances.

TABLE 1 Halftimes of the change in various parameters during the rise of tetanic tension measured under isometric or fixed-end conditions

Mode of contraction	$t_{1/2}$ Tension	Stiffness	10 Intensity	11 Intensity
		ms		
Fixed-end (n = 5)	49.4 ± 11.4	36.3 ± 8.8	33.2 ± 16.6	27.6 ± 12.1
Isometric (n = 8)	45.4 ± 16.1	31.2 ± 15.4*	27.0 ± 10.7	23.4 ± 11.5

All values measured from the time of the first stimulus. Mean halftimes are given ± SD.
*Measured under fixed-end conditions.

3. Intensity changes during relaxation

Relaxation occurs in two distinct phases in intact single fibers. The first is an almost isometric decline of force with a $t_{1/2}$ of ~1 s. The second phase develops after the "shoulder" of relaxation, and is rapid. This is associated with great sarcomeric disordering, and attempts to length-clamp this portion of relaxation were unsuccess-

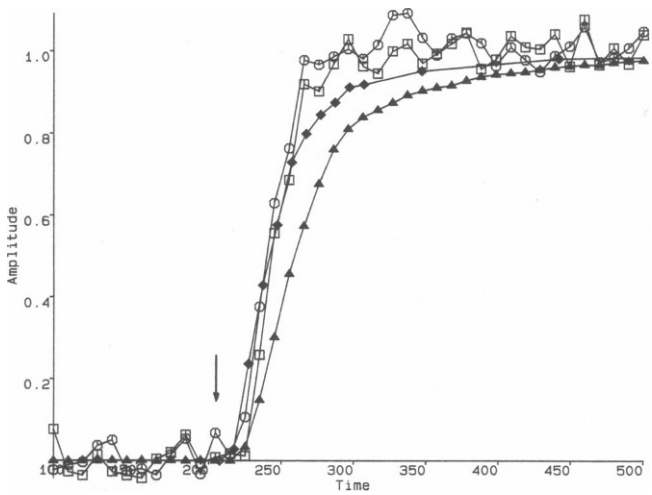

FIGURE 4 The time-resolved changes in tension (▲), stiffness (◆), and equatorial (10□; 11○) intensities during the rise of tetanic tension in a length-clamped tetanus. All traces have been normalized so that the value zero represents the resting level, the value one the level attained at the tetanus plateau. The 10 intensity change has been reversed for ease of comparison with other traces. In this and all subsequent figures showing time-resolved data, time zero represents the start of data acquisition. The arrow indicates the start of stimulation.

ful. As a result, the relaxation of the fiber was studied in the absence of a length clamp, since sarcomere length during the slow isometric phase remained constant even in the absence of length feedback. Because events during relaxation occur much more slowly than during activation, 25-ms sampling times were chosen in preference to 10 ms, to reduce the number of tetani required for averaging. The time courses of stiffness, tension, and equatorial intensity changes are shown in Fig. 5. It is apparent that although force declines during the isometric phase of relaxation, stiffness and equatorial intensities decay little from their values at the tetanus plateau. On average, the shoulder of tension occurred at a value of 0.64 P_0, and was accompanied by a decline of stiffness to 0.805 of its plateau value. The accompanying changes in I_{10} and I_{11} towards their resting values were 0.867 and 0.835 of their overall change respectively, at this point. After the "shoulder" all parameters return rapidly towards their resting values. On the whole, stiffness and equatorial intensities reached their resting values somewhat later than force.

4. Lattice spacing changes during tetani

On average, the lattice spacing at 2.15 μm sarcomere length was 39.4 nm in the relaxed state. When activated, unclamped fibers showed a lattice spacing increase which occurred with a time course similar to that of stiffness and intensity changes, that is leading the rise of tension (Fig. 6 *a*). Since the time-resolved sarcomere length signal was simultaneously recorded, it was possible to compute lattice volume during the tetanus as the product of the sarcomere length and the square of the lattice spacing (Fig. 6 *c*). This procedure would be expected to abolish changes in lattice spacing due to sarcomere shortening according to constant volume behavior, and this is what was observed, lattice volume expansion being much reduced in comparison to lattice spacing. In the majority of fibers, a gradual compression

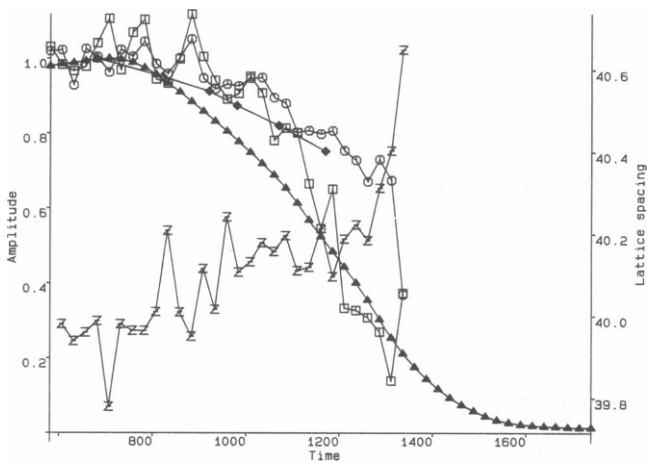

FIGURE 5 Lattice spacing (Z), stiffness (◆), equatorial intensities (10□; 11○), and force (▲) during relaxation. Average of 13 tetani. The base line represents the resting stiffness, and the intensities of the 10 and 11 reflections in the relaxed state. The data were gathered principally over the slow "isometric" phase of relaxation, hence the large lattice spacing change accompanying the fast second phase of relaxation is incomplete.

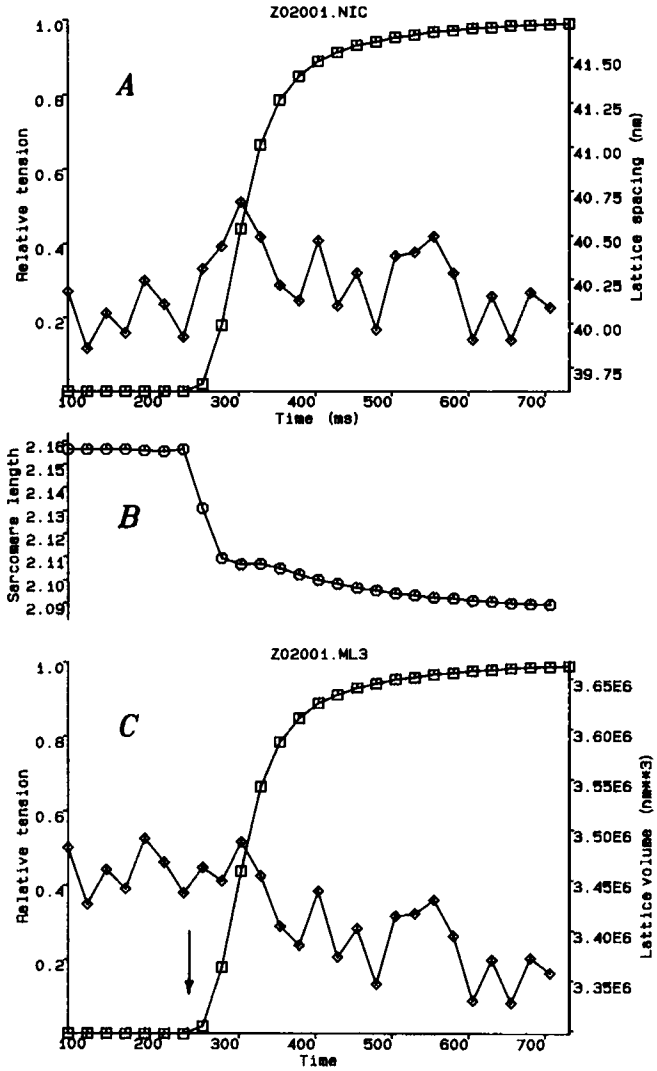

FIGURE 6 Lattice spacing (a; ◇) and volume (c; ◇) during the rise of tetanic tension (□) in a fiber not under length clamp control. In both cases the values of lattice spacing calculated from the 10 reflection have been used. All spacing dimensions are in nanometres. *b* shows the accompanying changes in sarcomere length (microns). Temperature 4°C, averaged over 22 tetani.

of the lattice could be observed after the initial expansion phase. This was not diminished when lattice volume was calculated. This effect is well seen in Fig. 7. The reciprocal of the square of lattice spacing is plotted versus sarcomere length during the tetanus rise in a fixed-end tetanus. On a plot of this kind, a constant volume relationship yields a straight line proportionality between the variables on the two axes. The dashed line represents constant volume behavior based on the lattice spacing and sarcomere length in the relaxed state. The sarcomere length and lattice spacing immediately before the onset of tetanic tension are represented by the points at the right-hand side of the figure. As tension develops, it can be seen that as the sarcomere length shortens during the rise of tension, the reciprocal of lattice spacing squared follows the constant volume relation until shortening is almost complete. There then follows a compression of the lattice during which the points deviate from the dashed line to lie above the predicted constant volume position on the left hand side of the figure.

In length-clamped fibers, the fast initial lattice expansion was greatly reduced, and in many cases was absent. However, the slow compression of the lattice was still apparent in both lattice spacing and lattice volume records in many fibers. A typical lattice spacing and lattice volume plot for the clamped fibers is seen in Fig. 8, *a* and *c*. The noise on the lattice spacing records results from the vertical expansion of the ordinate necessary to display spacing changes of only a few percent. The extent of lattice compression was 2% and had a slightly slower time course ($t_{1/2}$ ~60 ms) than force. A compression of the lattice has been observed in frog skinned fibers on going from the relaxed to the rigor state (Matsubara et al., 1984).

As described previously, relaxation occurred in two phases, a slow isometric phase followed by a rapid phase associated with a deterioration of sarcomere length homogeneity. During the isometric phase, lattice spacing remained constant or increased slightly (Fig. 5). During the second phase, large lattice spacing changes

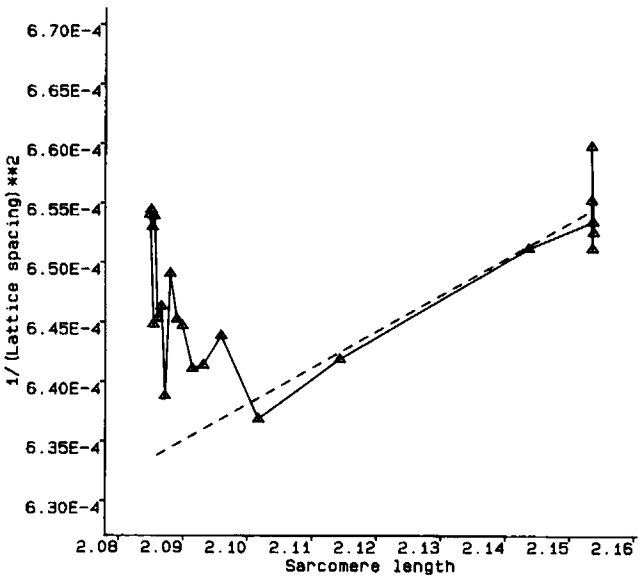

FIGURE 7 The reciprocal of lattice spacing squared versus sarcomere length during the tetanus rise. The dashed line shows the behavior of an ideal constant volume system, based on the lattice spacing and sarcomere length measured at rest. Temperature 4°C, average of 50 tetani.

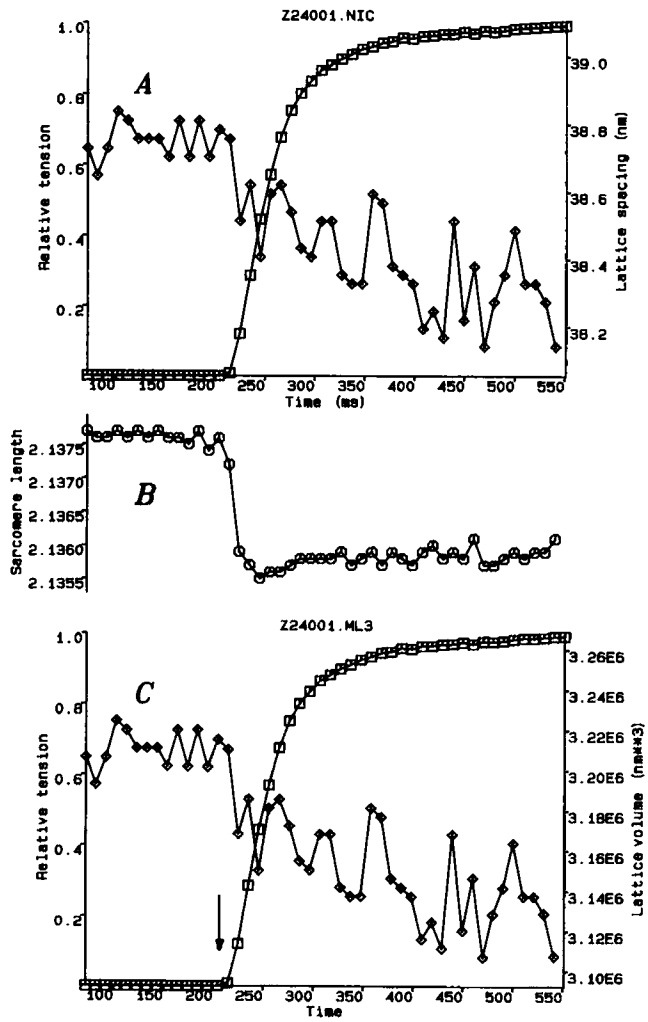

FIGURE 8 Lattice spacing (a; ◇) and volume (c; ◇) during the rise of tetanic tension (□) in a fiber under length clamp control. Accompanying sarcomere length changes (microns) are shown in *b*. All spacing dimensions in nanometers, average of 24 tetani.

occurred, which could either be an expansion or compression of the lattice.

DISCUSSION

Single muscle fibers offer a mechanically superior system for the study of muscle contraction. They permit more precise description of sarcomere and fiber lengths, and are suitable for length-clamping. They may also be dissected so as to minimize the effects of series compliance and optimize fiber orientation. Previous mechanical studies of the single fiber preparation have concentrated on the tibialis anterior muscle of *Rana temporaria,* so to relate the data presented here to previous findings as closely as possible, we have chosen to use this preparation for these x-ray diffraction studies. Many of the advantages of the single fiber for mechanical studies are also valid when applied to x-ray diffraction work. In particular, the single fiber preparation avoids the problems associated with the effects of a population of fibers present in whole muscle, wherein homogeneous kinetics of both mechanical and structural events can occur, as well as in terms of sarcomere length and activation. In addition, the viability of the preparation is evident and capable of being accessed throughout the experiment. Visual inspection of the fiber at the end of the experiments reported here showed no sign of beam damage, and the laser diffraction pattern from the fiber did not alter during the course of an experiment. We conclude that electrical or mechanical failure of the fiber preceeds failure due to beam damage. In whole muscle work, beam damage is indicated by a gradual decline in tetanic tension, whereas the single fiber preparation showed no more than a few percent change in tetanic tension during the course of an experiment. Thus the proven viability of the single fiber preparation during x-ray diffraction studies (as opposed to whole muscle) shows its suitability for further studies of structural events accompanying contraction. We have found that although the x-ray diffraction pattern from the single fiber is weaker than that from whole muscle because of the smaller mass available to scatter the beam, the definition of individual reflections is better than that obtained either from whole muscle or from skinned fibers, and its survivability in the beam is excellent.

The relaxed pattern from a single fiber shows features which are not clearly observed in the whole muscle preparation. In particular, the Z-line reflection and the 20 reflection are well defined on either side of the 11 peak. This suggests a high degree of ordering within the structure of the fiber. During activation, these reflections become masked by the broadening of the 11 reflection. The 10:11 intensity ratio obtained in this study is quite similar to that reported by Matsubara and Yagi (1978). The slightly smaller value of the ratio at the tetanus plateau in our experiments (0.50) may be due to a more complete stimulation of our preparation than is possible with whole muscle, where some fibers may not be stimulated and therefore tend to cause the ratio to be somewhat higher than expected. Haselgrove and Huxley (1973) were aware of this problem, and corrected their data accordingly, but still obtained a higher ratio (0.78) than that reported here for the tetanus plateau. Similarly, the sarcomere length of the activated whole muscle preparation cannot be so precisely defined as in the single fiber preparation.

Some of our experiments have been performed under length-clamped conditions in contrast to all earlier studies of time-resolved x-ray diffraction changes during contraction, where sarcomere length changes were not monitored and certainly not controlled during activation. Why is it necessary to clamp sarcomere length during such time-resolved studies as these? Changes in sarcomere length during the tetanus rise are known to reduce the rate of tension development, produce changes in lattice spacing, and may introduce an isotonic equatorial intensity distribution into the equatorial pattern observed during the tetanus rise. In addition, the equatorial intensity has a static dependence on sarcomere length, as shown in Fig. 3. In healthy fibers, at sarcomere lengths on the plateau of the length-tension relationship, and with suitable precautions to reduce tendon compliance, sarcomere length changes during the tetanus rise may be reduced to 2–3%. However, length-clamping permits this change of sarcomere length during activation to be reduced by 90%, and hence the influence of sarcomere length changes to be minimized, and the conditions of measurement more precisely defined. The effectiveness of the length clamp can be judged in the reduction of lattice expansion during the tetanus rise that is observed under length clamp control (see Figs. 6 and 8).

Under length clamp, the time course of intensity changes during the tetanus rise is similar for 10 and 11 reflections. Initial experiments suggested a lead of 10 over 11 in some fibers, but subsequently it was found that under length-clamped conditions no such phenomenon could be identified within the resolution of our measurements (10 ms). As described earlier, Kress et al. (1986) obtained a mean difference in halftimes between I_{11} increase and tension of 11 ms during the tetanus rise in whole muscle, whereas mechanical measurements by Cecchi et al. (1982) showed a 15-ms lead of stiffness over tension, also during the tetanus rise, but in the single fiber preparation. We report here a somewhat larger

difference in halftimes for the equatorial changes and force, 20 ms in length-clamped fibers. Inspection of Fig. 5 of Matsubara and Yagi (1978) shows a similar lead of intensity changes over tension. On average we found intensity changes lead stiffness, but given the time resolution of our present measurements and the fact that stiffness measurements were performed under fixed-end conditions, we believe the time course of the intensity changes and stiffness rise can be regarded as effectively identical. The onset of tension development and of the changes in stiffness and equatorial intensities seemed comparable, within the limits of our sampling rate (10 ms). It would therefore be reasonable to assume that they represent the same event, i.e., cross-bridge (S1) attachment. Furthermore, if the reflection intensities are proportional to the number of attached bridges, then the parallel time course of stiffness and tension suggests that the stiffness of the attached, low-force cross-bridge is the same as that of the attached bridges at the tetanus plateau, and supports the view, at least in the intact fiber, that stiffness is proportional to the number of attached cross-bridges. It has been proposed that the lead of stiffness over tension results from a stronger binding of "weakly bound" cross-bridge states (Brenner, 1990). However Schoenberg (1988) has reported that in relaxed skinned fibers at physiological ionic strength, the proportion of attached weakly bound bridges is unlikely to be $>5\%$ in frog. More recently, Schoenberg (1991. *Biophys. J.* 59:51a) suggests that 2-kHz stiffness measurements should detect 88% of the stiffness due to weakly bound bridges in the relaxed state. We calculate that at 4 kHz (the frequency of our length sinusoid) the fraction detected should be 92%, and therefore a slowing of rate constants governing the equilibrium between bound and unbound states at a constant affinity would not result in a marked increase in stiffness. Hence, to account for our lead of stiffness over tension, a substantial increase in affinity of the binding of weak states in the presence of calcium ions would be required. Some groups have measured such an increase (Wagner and Stone, 1983), whereas others report a more modest effect (Chalovich and Eisenberg, 1986). El-Saleh and Potter (1985), working at physiological ionic strength, found essentially no increase in binding affinity of the weakly bound states to actin in the presence of calcium ions. Furthermore, since the change in the equatorial reflections on the formation of weak bridges in frog muscle occurs primarily in the 11 reflection at low ionic strength (Xu et al., 1986) while our data shows a parallel change in 11 and 10 reflections, we believe that the lead of stiffness during the tetanus rise arises principally from the formation of a low force, strongly bound cross-bridge state. Several more detailed explanations of the existence of low-force bridges have been offered in the past (Ford et al., 1986; Bagni et al., 1988) which cannot be distinguished in terms of the data presented here.

Relaxation occurs in two phases, a slow isometric phase followed by a rapid phase of sarcomeric disorder. The slow phase occurs with little decline in stiffness or reversal of equatorial intensities. Such change as does occur has a time course much slower than force. The event that limits the rate of relaxation under isometric conditions is now known. The dissociation rate constant of calcium from troponin is relatively fast (200 s^{-1}), at least from the low-affinity calcium-binding sites, which are thought to be responsible for regulation. In contrast, the decline of tension occurs with a rate constant more like 1 s^{-1}. The decline of the aequorin light transient at the end of a tetanus occurs very quickly, but there is some evidence of a tailing of this response, suggesting that the true levels of free calcium may be approached rather more slowly (Cannell, 1986). The presence of parvalbumins in frog muscle in appreciable amounts (1 mM) has been proposed to influence the rate of relaxation, though this action is controversial and may be rather complex (Gillis, 1982; Griffiths et al., 1990). Alternatively, the relaxation rate constant is not dissimilar to the cross-bridge cycling rate, and may therefore indicate that inhibition of actin–myosin interaction of an individual bridge can only occur after that bridge has returned to the start of its cycle. However, both the x-ray data and the stiffness measurements indicate an elevated level of cross-bridge attachment compared with force during isometric relaxation, which implies that once again there is a shift in the population of attached cross-bridges towards a low force but strongly binding cross-bridge state.

Lattice spacing changes in the unclamped fiber agree reasonably well with sarcomere length changes to yield constant volume behavior during the development of tetanic tension. The lead of lattice expansion over tension during the tetanus rise in unclamped fibers would be expected if some exponential series compliance were present in the system since the bulk of the extension of the exponential compliance would occur over a low force range, and hence in the earlier part of the tetanus rise. That the lattice expansion is much reduced when expressed as lattice volume supports this view. Under length-clamped conditions, such an expansion was generally absent. A compression of the lattice was frequently observed of much slower time course than the expansion, and was not reduced when expressed in terms of lattice volume. The compression amounted to 2% of the resting lattice spacing and occurred with a $t_{1/2}$ of ~ 60 ms. If the distance between

the core of the myosin and adjacent actin filaments is $3^{-1/2}$ times the myosin spacing, and if this is 39 nm, then a 2% compression represents a 0.5-nm approach of actin and myosin filaments. The lattice compression, observed under length-clamp control, represents the first direct observation of the lattice compression expected from a radial compression component of cross-bridge force, predicted by certain models of attached cross-bridge structure (Schoenberg, 1980*a*, *b*). In skinned fibers, a compression of the filament lattice has been reported during the development of active tension (Brenner and Yu, 1983, 1985). However, a similar degree of lattice compression was observed in skinned fibers on entering the rigor state (Matsubara et al., 1984) where cross-bridge attachment would be close to 100% but longitudinal tension would be small. A more detailed description of this lattice compression will be presented in a subsequent publication dealing with the response of the fiber to rapid length changes.

The authors are indebted to the staff of the EMBL outstation for their assistance in this project.

Supported by EMBO, NIH, and MRC.

REFERENCES

Adrian, R. H. 1956. The effect of internal and external potassium concentration on the membrane potential of frog muscle. *J. Physiol. (Lond.)*. 133:631–658.

Bagni, M. A., G. Cecchi, and M. Schoenberg. 1988. A model of force production that explains the lag between cross-bridge attachment and force after electrical stimulation of striated muscle fibers. *Biophys. J.* 54:1105–1114.

Brenner, B. 1990. Muscle mechanics and biochemical kinetics. *Top. Mol. Struct. Biol.* 13:77–150.

Brenner, B., and L. C. Yu. 1983. Equatorial x-ray diffraction from single skinned rabbits psoas fibers during various degrees of activation. *Biophys. J.* 41:257a. (Abstr.)

Brenner, B., and L. C. Yu. 1985. Evidence for a radial cross-bridge compliance with equilibrium position at 380 Å. *Biophys. J.* 47:382a. (Abstr.)

Cannell, M. B. 1986. Effect of tetanus duration on the free calcium during relaxation of frog skeletal muscle fibers. *J. Physiol. (Lond.)*. 376:203–218.

Cecchi, G., F. Colomo, and V. Lombardi. 1976. A loudspeaker servo-system for determination of mechanical characteristics of isolated muscle fibres. *Bol. Soc. Ital. Biol. Sper.* 52:733–736.

Cecchi, G., P. J. Griffiths, and S. R. Taylor. 1982. Muscular contraction: kinetics of cross-bridge attachment studied by high frequency stiffness measurements. *Science (Wash. DC)*. 217:70–72.

Cecchi, G., P. J. Griffiths, and S. R. Taylor. 1986. Stiffness and force in activated frog skeletal muscle fibers. *Biophys. J.* 49:437–451.

Cecchi, G., F. Colomo, V. Lombardi, and G. Piazzesi. 1987. Stiffness of frog muscle fibres during rise of tension and relaxation in fixed-end or length-clamped tetani. *Pfluegers Arch. Eur. J. Physiol.* 409:39–46.

Chalovich, J. M., and E. Eisenberg. 1986. The effect of troponin–tropomyosin on the binding of heavy meromyosin to actin in the presence of ATP. *J. Biol. Chem.* 261:5088–5093.

Eason, G. 1989. On the impulsive loading of muscle fibres. *J. Sound Vib.* 133:163–171.

Elliott, G. F., J. Lowy, and C. R. Worthington. 1963. An X-ray and light diffraction study of the filament lattice of striated muscle in the living state and in rigor. *J. Mol. Biol.* 6:295–305.

El-Saleh, S. C., and J. D. Potter. 1985. Calcium-insensitive binding of heavy meromyosin to regulated actin. Interaction under physiological ionic strength. *J. Biol. Chem.* 259:11014–11021.

Ford, L. E., A. F. Huxley, and R. M. Simmons. 1978. Tension responses to sudden length changes in stimulated frog muscle fibres near slack length. *J. Physiol. (Lond.)*. 269:441–515.

Ford, L. E., A. F. Huxley, and R. M. Simmons. 1986. Tension transients during rise of tetanic tension in frog muscle fibres. *J. Physiol.* 372:595–609.

Gillis, J. M., D. Thomason, J. Lefevre, and R. H. Kretsinger. 1982. Parvalbumins and muscle relaxation: a computer simulation study.

Griffiths, P. J., J. J. Duchateau, Y. Maeda, J. D. Potter, and C. C. Ashley. 1990. Mechanical characteristics of skinned and intact muscle fibres from the giant barnacle, *Balanus nubilus*. *Pfluegers Arch. Eur. J. Physiol.* 415:554–565.

Hanson, J., and H. E. Huxley. 1955. The structural basis of contraction in striated muscle. *Symp. Soc. Exp. Biol.* 9:228–269.

Haselgrove, J. C. 1975. X-ray evidence for conformational changes in the myosin filaments of vertebrate striated muscle. *J. Mol. Biol.* 92:113–143.

Haselgrove, J. C., and H. E. Huxley. 1973. X-ray evidence for radial cross-bridge movement and for the sliding filament model in actively contracting skeletal muscle. *J. Mol. Biol.* 77:549–568.

Hendrix, J., H. Fuerst, B. Hartfiel, and D. Dainton. 1982. A wire per wire detector system for high counting rate X-ray experiments. *Nucl. Instr. Methods.* 201:139–144.

Huxley, A. F. 1957. Muscle structure and theories of contraction. *Prog. Biophys.* 7:255–318.

Huxley, A. F., and V. Lombardi. 1980. A sensitive force transducer with resonant frequency 50 kHz. *J. Physiol. (Lond.)*. 305:15–16P.

Huxley, A. F., and R. Niedergerke. 1954. Structural changes in muscle during contraction: interference microscopy of living muscle fibres. *Nature (Lond.)*. 173:971–973.

Huxley, A. F., and R. M. Simmons. 1971. Proposed mechanism of force generation in striated muscle. *Nature (Lond.)*. 213:533–538.

Huxley, H. E., and J. Hanson. 1954. Changes in the cross-striations of muscle during contraction and stretch and their structural interpretation. *Nature (Lond.)*. 173:973–976.

Huxley, H. E., and J. C. Haselgrove. 1977. The structural basis of contraction in muscle and its study by rapid X-ray diffraction methods. *In* Myocardial Failure. G. Riecker, A. Weber, and J. Goodwin, editors. 4–15.

Kress, M., H. E. Huxley, A. R. Faruqi, and J. Hendrix. 1986. Structural changes during activation of frog muscle studied by time-resolved X-ray diffraction. *J. Mol. Biol.* 188:325–342.

Maeda, Y., C. Boulin, A. Gabriel, I. Sumner, and M. H. J. Koch. 1986. Intensity increases of actin layer-lines on activation of the Limulus muscle. *Biophys. J.* 50:1035–1042.

Matsubara, I., and N. Yagi. 1978. A time-resolved X-ray diffraction study of muscle during twitch. *J. Physiol. (Lond.)*. 278:297–307.

Matsubara, I., Y. E. Goldman, and R. M. Simmons. 1984. Changes in the lateral filament spacing of skinned muscle fibers when cross-bridges attach. *J. Mol. Biol.* 173:15–33.

Schoenberg, M. 1980*a*. Geometrical factors influencing muscle force development. 1. The effect of filament spacing upon axial forces. *Biophys. J.* 30:51–68.

Schoenberg, M. 1980*b*. Geometrical factors influencing force development: 2. Radial forces. *Biophys. J.* 30:69–78.

Schoenberg, M. 1988. Characterization of the myosin adenosine triphosphate (M.ATP) cross-bridge in rabbit and frog skeletal muscle fibres. *Biophys. J.* 54:135–148.

Schoenberg, M. 1991. Mechanical detection of weakly-binding M-ATP crossbridges. *Biophys. J.* 59:51a. (Abstr.)

Wagner, P. D., and D. B. Stone. 1983. Calcium-sensitive binding of heavy meromyosin to regulated actin requires light chain 2 and the head–tail junction. *Biochemistry.* 22:1334–1342.

Xu, S., M. Kress, and H. E. Huxley. 1987. X-ray diffraction studies of the structural state of crossbridges in skinned frog sartorius muscle at low ionic strength. *J. Muscle Res. Cell Motil.* 8:39–54.

Yu, L. C., R. W. Lymn, and R. Podolsky. 1977. Characterization of a nonindexible equatorial X-ray reflection from frog sartorius muscle. *J. Mol. Biol.* 115:455–464.